# Transport properties of a shunted surface superlattice in an external magnetic field

T. Feil, C. Gerl, and W. Wegscheider
*Institut für Experimentalphysik, Universität Regensburg, 93040 Regensburg, Germany*
(Received 21 October 2005; revised manuscript received 27 December 2005; published 1 March 2006)

We study the transport through a shunted surface superlattice system in the presence of an external magnetic field. Such a system consists of a weakly doped, instability free superlattice (shunt) that is overgrown on the edge with a two-dimensional electron system (surface superlattice). A magnetic field parallel to a static applied electric field along the superlattice axis induces current resonances in the shunt characteristics which are explained by Stark-cyclotron resonances. These resonances support the conclusion that the field alignment in the shunted surface superlattice structure is homogeneous. An increasing magnetic field perpendicular to the transport direction leads to characteristic crossings of the current-voltage characteristics of both shunt and surface superlattice. They are explained by a semiclassical model which assumes a competition between the magnetic and electric localization of the miniband electrons. We conclude that our structure indeed presents a domain free high density superlattice and might therefore be a promising candidate for the realization of an active electrically driven Bloch oscillator.

DOI: 10.1103/PhysRevB.73.125301 PACS number(s): 73.50.Fq, 75.70.Cn, 72.20.My, 73.50.Jt

## I. INTRODUCTION

Based on the seminal work of Esaki and Tsu,[1] predicting negative differential conductivity (NDC) in a superlattice (SL) due to Bloch oscillations, Ktitorov *et al.*[2] showed that the superlattice acts as a gain medium for all frequencies up to the Bloch frequency. Many of the early predictions for superlattices have been demonstrated experimentally, including the formation of Wannier-Stark ladders in biased SLs,[3] the direct observation of Bloch oscillations with the help of time domain spectroscopy,[4–6] and the resolution of terahertz (THz) resonances in the photoconductivity of a biased SL.[7] Moreover, theoretical results by Willenberg *et al.*[8] extend the Ktitorov results to a wide range of SL parameters and electric field and temperature regions. Experimental evidence for the predicted gain in SLs was recently given by a derivation of the dynamic conductivity from time domain spectroscopy results[9] and by a direct observation of the crossover from loss to gain in a biased super-SL structure.[10]

An active oscillator based on the SL gain both predicted theoretically and experimentally has two main requirements. The electric field across the device needs to be homogeneous and the gain, given by the real part of the dynamic conductivity, must be large enough to overcome waveguide losses. A large conductivity requires high carrier densities. Unfortunately, these highly doped samples are subject to electric field instabilities due to charge accumulation inside the sample. The origin of these instabilities is a negative differential drift velocity which results in SLs from the electron motion in a cosine-shape miniband. For small electric fields the electron distribution picks up an average positive drift velocity, however, scattering is so strong that the nonlinearity of the miniband dispersion is not felt by the electrons. For increasing electric field the electrons eventually reach the nonlinear parts of the dispersion and the drift velocity starts to saturate. Then, for very large electric fields, electrons reach the Brillouin zone boundary and undergo Bragg reflection. This leads to an oscillatory motion of the electrons referred to as Bloch oscillations. Since more and more electrons perform Bloch oscillations with increasing electric field, the drift velocity continuously decreases. For high electron densities this negative differential drift velocity leads to strong electric field inhomogeneities in SLs.[30] However, Bloch gain in SLs is only predicted for homogeneous electric field distributions. Thus, the first major step towards a Bloch oscillator is to reconcile a homogeneous electric field distribution along the SL with high carrier densities. In Ref. 11 we introduced a SL/shunt structure in which a surface SL (SSL) is in direct lateral contact to a shunt, which provides electric field stabilization[12] to the SSL even in the high electron density regime. The main claims made for the shunted SSL structures are that the electric field across the shunt is very close to homogeneous and that the NDC observed in the SSL characteristics is due to stable electrically excited Bloch oscillations.

In this paper we study the transport through one of these structures in the presence of an external magnetic field. For conventional superlattices both the magnetic field alignment along the SL axis and perpendicular to it have been investigated theoretically[13–20] and experimentally.[21–25] Depending on the mobility inside the SL quantum wells, electrons are Landau localized by a magnetic field along the SL axis. If this localization occurs, the transport channels along the device become essentially one dimensional which leads to a strong suppression of the overall current.[17] Moreover, elastic and quasielastic scattering between different Wannier-Stark-Landau levels in neighboring wells opens up additional transport paths when the potential difference between different wells equals the cyclotron energy. In every such situation the current through the SL takes on a maximum, leading to a series of resonances which are referred to as Stark-cyclotron resonances (SCR).[13,22] The current-voltage characteristics of the shunt show both a strong overall transport reduction and SCRs. From the latter we can directly comment on the electric field distribution in the SL-shunt system.

When a magnetic field perpendicular to the SL axis is applied, the semiclassical transport theory shows that both the magnetic and the electric field can localize the electrons

 

along the transport direction.[20] For small electric fields the additional magnetic confinement leads to a smaller drift velocity of the system, resulting in a positive magnetoresistance (MR). However, for strong electric localization the magnetic field can actually cause an increased drift velocity and, hence, a negative MR. This change from positive to negative MR leads to a distinct crossing of the current-voltage characteristics of a SL and a number of transport properties like the scattering time and the perpendicular effective mass can be extracted from this behavior. Especially, since the semiclassical theory based on Bloch oscillations predicts a linear shift of the negative differential resistance peak of the superlattice[19,24] as compared to a quadratic one for resonant tunneling,[26] the transport regime can be determined experimentally.

For SSLs there are actually three distinct magnetic field directions due to its reduced dimensionality. We will consider here only a magnetic field in the plane of the two-dimensional electron system, since the high mobility for perpendicular alignment leads to strong Landau quantization, which is not covered by the semiclassical model.[27]

The paper is organized in the following way. In Sec. II we collect the theoretical results with which the experimental data will be explained. This is followed by a brief review of the sample structure and its working principle in Sec. III. The experimental results are then presented and analyzed in Sec. IV and the paper ends with conclusions and a summary in Sec. V.

## II. THEORY

When a magnetic field $B$ is applied in parallel with a static electric field $F$ along the axis of a superlattice the system becomes completely quantized.[13–16] The magnetic field leads to Landau quantization within the superlattice layers, whereas the electric field along the SL leads to the formation of an equidistant Stark ladder. Thus, a set of equidistant ladder states, the so-called Wannier-Stark-Landau (WSL) levels, sits in each SL well, as shown in Fig. 1(a). When the states in neighboring wells sit at different energies, transport occurs by electrons hopping along the lowest lying states in each well. This situation is similar to the Wannier-Stark hopping in the magnetic field free case. But once WSL states in neighboring wells become degenerate, elastic processes followed by inelastic relaxation can open new transport paths through the SL [arrows in Fig. 1(a)]. These additional paths lead to an increased transport. Therefore, the degeneracy of the WSL levels leads to a series of current peaks which are referred to as Stark-cyclotron resonances. The condition for the degeneracy is given by

$$\nu eFd = n\hbar\omega_C, \quad \nu = 0, \pm 1, \ldots, \; n = 0, 1, \ldots, \tag{1}$$

where $eFd$ is the Stark splitting, the potential drop caused by the field $F$ over one SL period $d$, and $\hbar\omega_C = \hbar eB/m$ is the cyclotron energy. By comparison of the ratios between different slopes of the SCRs the values $\nu$ and $n$ can usually be assigned unambiguously to each resonance. Then, when the effective mass $m$ is known, information about the electric field alignment in the superlattice structure can be made.

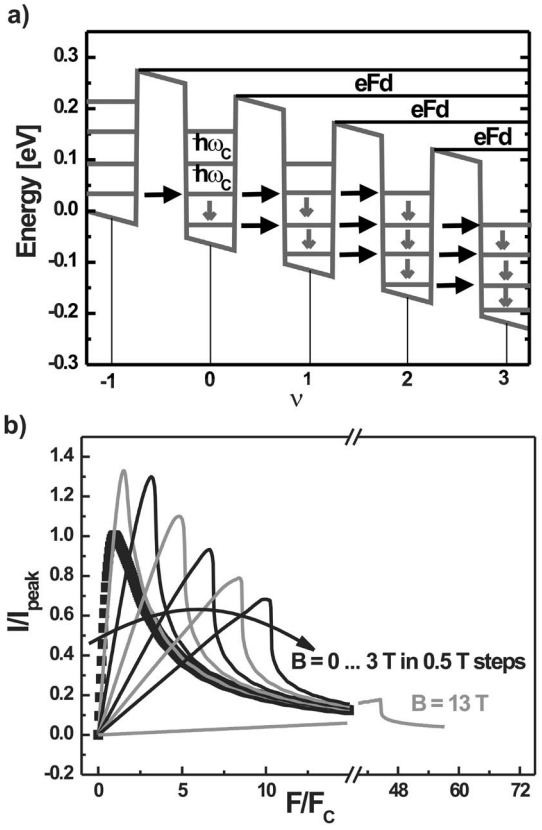


FIG. 1. (a) Schematic drawing of possible transport channels resulting in SCRs. (b) Numerical results for miniband transport in a superlattice in the presence of a perpendicular magnetic field.

For a magnetic field alignment perpendicular to the superlattice axis the mobility is usually not large enough to lead to Landau quantization. Therefore, transport in this situation is described on the basis of the semiclassical theory introduced by Esaki and Tsu.[1,23–25]

Assuming the transport to flow along the $x$ direction, whereas the magnetic field is applied along the $z$ direction, the semiclassical acceleration theorem results in

$$\frac{\partial k_x}{\partial t} = \frac{eF}{\hbar} + \frac{eB}{m_{\|}} k_y(t), \tag{2}$$

$$\frac{\partial k_y}{\partial t} = -\frac{eB}{m_{\perp} d} \sin[k_x(t)d], \tag{3}$$

where $m_{\|}$ is the effective mass of the movement in the SL planes, and $m_{\perp} = 2\hbar^2/\Delta d^2$ is the zone center effective mass along the SL direction in a miniband of width $\Delta$. The drift velocity, which is proportional to the current, can then be calculated according to[1]

$$v_d = \frac{\hbar}{\tau m_{\perp} d} \int_0^{\infty} e^{-t/\tau} \sin[k_x(t)d] dt, \tag{4}$$

assuming an electron scattering time $\tau$. For general values of the magnetic and electric field, the system can only be solved numerically. Assuming a scattering time of 1 ps and the ef-

fective mass $m_{||}$ to be that of GaAs, the drift velocity for different magnetic fields is plotted in Fig. 1(b). There, the electric field is given in units of the critical field $F_C = \hbar/ed\tau$. For zero magnetic field, the drift velocity initially increases linearly before it saturates and is followed by a region of negative differential conductivity, when more and more electrons start to perform Bloch oscillations. With the magnetic field turned on, this basic shape survives, but also a typical crossing of the transport characteristics can be observed. Each trace shows a low bias region with positive MR and a large bias regime with negative MR. Detailed numerical investigations[25] predict that in the limit $B \to 0$ the crossover field between positive and negative MR is at $F = F_C/2$. Moreover, the position of the negative differential resistance peak in the electric and magnetic field plane is predicted[19,24] to be found at $B = \sqrt{(m_{||}/2\Delta)}F_C$.

In the limit $F/F_C \ll B/B_0$, where $B_0 = \sqrt{m_\perp m_{||}}/e\tau$, the above equations possess a closed form solution[25] according to

$$v_d = \frac{\mu F}{1 + \left(\frac{B}{B_0}\right)^2}, \tag{5}$$

which can be rewritten as

$$\frac{R}{R_0} = 1 + \left(\frac{B}{B_0}\right)^2, \tag{6}$$

where $R = V/I$ and $R_0$ is the resistance for $B \to 0$. This latter expression allows us to deduce $B_0$ experimentally by a linear fit of the resistance versus the square of the magnetic field.

From the NDC peak position at $B = 0$, from the shift of the NDC peak with magnetic field, and from a linear fit of the resistance for large magnetic fields we can deduce all relevant transport parameters. With these we can then go back and evaluate the described model and compare the results with the experiment.

## III. THE DEVICE

The investigated sample [cf. Fig. 2(a)] consists of a $GaAs/Al_{0.3}Ga_{0.7}As$ SL of 66 periods of 12 nm wide wells and 3 nm wide barriers that has two contact layers on each side. This structure is *in situ* cleaved and overgrown on the side with a 5 nm wide GaAs well, referred to as the cleaved-edge well (CEW), followed by a 2000 nm thick $Al_{0.3}Ga_{0.7}As$ barrier and a highly doped gate contact. The lateral width [$z$ axis in Fig. 2(a)] of the sample is 500 $\mu$m. More details of the sample preparation technique are given elsewhere.[11,28] When no gate voltage is applied, only the current through the undoped SL, in the following referred to as the shunt, is measured. The unintentional doping in the shunt leads to a small $nL$ product with domain free, monotonically increasing transport.[29,30] For a positive gate voltage, a two-dimensional electron system is established in the CEW which is strongly modulated by the undoped SL. The strong modulation leads to the formation of minibands and minigaps similar to the situation in a conventional SL. The miniband structure of the surface SL can be calculated with the help of two-dimensional self-consistent simulations[11] and is plotted for two different densities in the inset of Fig. 2(c), in which also the widths of the lowest minibands are given. Thus, for positive gate bias both the current through the shunt and the SSL are measured. The difference between both traces is the transport contribution from the SSL. The current follows the shape predicted for a SL with homogeneous field alignment and is in good agreement with a theoretical fit from a simple semiclassical model.[1] In Fig. 2(c) the device characteristics at 4.2 K for a SSL density of $1.7 \times 10^{11}$ cm$^{-2}$ are shown. From the position of the NDC peak the scattering time $\tau$ can be deduced according to $\tau = \hbar/eF_C d$. This allows one then to estimate the ratio between half the miniband width $\Delta/2$ and the scattering induced broadening $\hbar/\tau$. From a comparison of this value to the quantum-mechanical results presented in Ref. 31 the SL transport regime can be deduced. As Fig. 2(b) shows, the studied samples operate in the miniband transport regime, which crosses over into the Wannier-Stark ladder hopping regime for Stark-splittings $eFd$ larger than $\Delta$. It might be argued that our observations, despite these numbers, are dominated by resonant tunneling processes. This can, however, also be excluded due to the observation of Shubnikov-deHaas oscillations at 4.2 K for magnetic fields below 1 T.

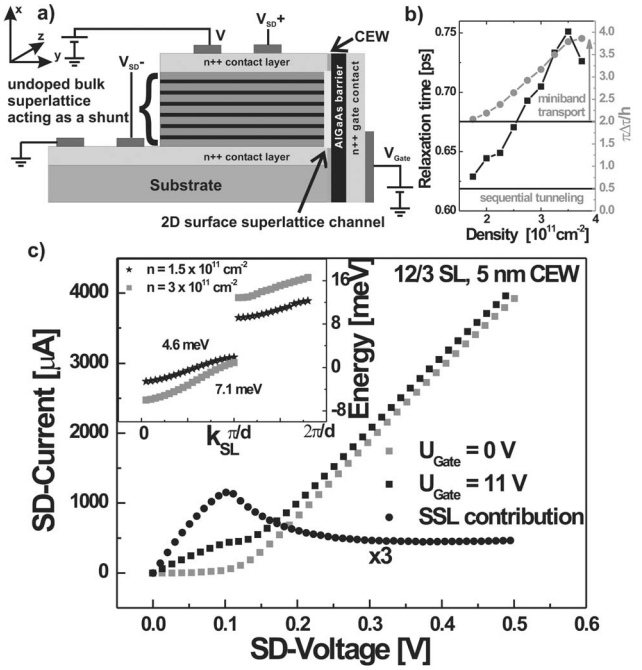


FIG. 2. (a) Schematic drawing of the sample structure. (b) Relaxation times and transport regimes. (c) Transport contributions in the sample structure. The inset shows the SSL band structure for two different densities.

## IV. EXPERIMENT

This section is divided into two parts. First, we study the transport through the shunt for a magnetic field aligned parallel to the SL axis. From the corresponding results, important information about the homogeneity of the electric field

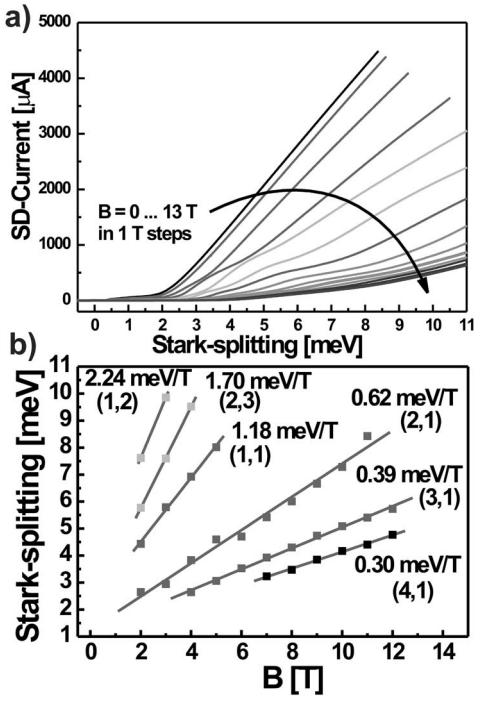


FIG. 3. (a) Current-voltage traces of the shunt for several magnetic field values applied parallel to the current. (b) Positions of magnetic field-induced features of the traces in (a).

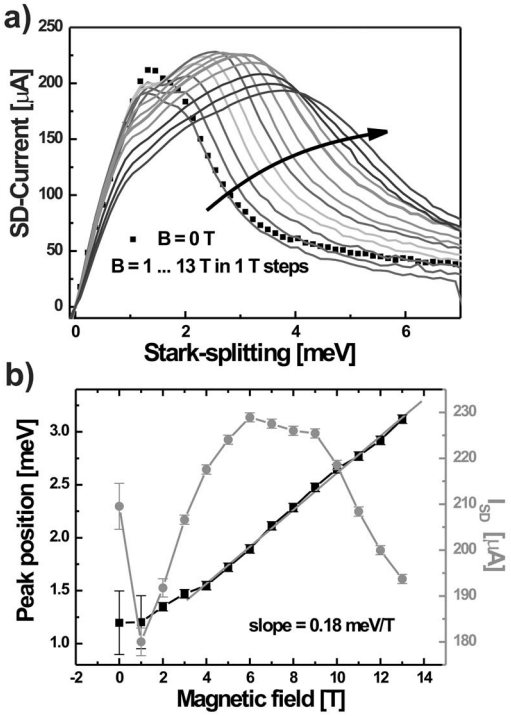


FIG. 4. (a) Current-voltage characteristics of the described SSL at a density of $1.7\times10^{11}$ cm$^{-2}$ for magnetic fields from 1 to 13 T (lines). Also the $B=0$ trace is shown (symbols). (b) Position and height of the NDC peak of the data in panel (a).

across the shunt can be deduced. In the second part the SSL transport is investigated for a magnetic field which is both perpendicular to the SL axis and in the plane of the two-dimensional electron system. From these measurements important system parameters are extracted and are then used to calculate current-voltage characteristics according to the model described in the preceding section.

Figure 3(a) shows the current-voltage characteristics of the shunt for a number of magnetic fields ranging from 0 to 13 T and being aligned parallel to the electric field. Two distinct transport changes can be observed. Both a strong suppression of the total current, resulting from the formation of one-dimensional transport channels,[17] is observed and a number of peak structures become visible in these current traces. A detailed analysis of the derivatives $dI/dV$ and $d^2I/dV^2$ shows a series of clear peaks whose positions are plotted versus the applied magnetic field in Fig. 3(b). A linear dependence for these features is found as expected from Eq. (1) and a comparison of the slopes allows an unambiguous assignment of values $(\nu,n)$ to these lines [also shown in Fig. 3(b)]. For an effective mass of about 0.07 $m_e$ in the 12 nm wide well, a cyclotron energy of about 1.6 meV/T is found. At the same time, a value of 1.18 meV/T for the slope of the (1,1) SCR transition is extracted from Fig. 3(b). Both values should be equal when 100% of the shunt is aligned homogeneously. From their ratio, we can deduce that a homogeneous electric field alignment is found across a minimum of about 75% of the shunt. Due to a possible misalignment of the magnetic field, which would lead to a smaller cyclotron energy, the 75% represents a lower limit. Moreover, since there are no intrinsic buffer layers between SL and contact, a spill over of electrons in a number of SL periods can be expected which suggests that an even larger part of the shunt is perfectly aligned. Since the electric field distribution across the shunt is not completely known, it is difficult to estimate how the SSL transport is influenced by this. Although a worst case scenario would mean that the Stark splittings given below have to be reduced by about 25%, this is unlikely since at least part of this reduction is compensated by a somewhat inhomogeneous electric field across a short section of the shunt. This section has to be present in order to avoid NDC in the current-voltage characteristic.[30] Despite this remaining uncertainty, the observation of SCRs in the shunt characteristics strongly supports the first claim of a close to homogeneous electric field alignment for the shunted SSL system. Since the lateral extension of the SSL is only about 10 nm, the field across the SSL will look similar to the one across the shunt.[12]

When the magnetic field is applied perpendicular to the current direction, the shunt characteristics show a typical crossing behavior that has been observed before[23,25] and is again in agreement with the assumption that the electric field alignment is close to homogeneous. However, for the shunt and all other SLs studied so far, the connection between the measured current-voltage characteristics and the drift velocity as calculated in Fig. 1 could only be established through the additional solution of the Poisson and continuity equations.[20] This is no longer necessary for the SSL. It directly shows the NDC expected for a homogeneously aligned high-density superlattice.

In Fig. 4(a) we plot the evolution of the current-voltage characteristic of the SSL for a density of $1.7\times10^{11}$ cm$^{-2}$

with the magnetic field in the plane of the two-dimensional system and perpendicular to the transport direction. The traces show an initial current shoulder which appears right where the shunt transport sets in. The transport characteristics of SSLs without shunt exhibit no stable NDC and also a larger transport than those with shunt[11] at $B=0$ T. This can explain why the SSL current decreases, at least for smaller magnetic fields, beyond the initial shoulder. When we plot in Fig. 4(b) the position and the height of the NDC peak in dependence of the magnetic field, the qualitative behavior is in good agreement with the theoretical predictions in Fig. 1. The peak current first increases with magnetic field, then reaches a maximum before it continuously decreases. It is not clear yet why the $B=0$ value deviates from this behavior. The peak positions have been extracted assuming a series resistance of about 150 Ω, a value consistent with the sheet resistivity and the geometry of the contact layers. A clear linear relationship between the magnetic field and the NDC peak position is found (independent of the series resistance). This linear dependence contradicts the assumption that a resonant tunneling process underlies the observed NDC. Resonant tunneling predicts a quadratic shift of the peak position with the $B$ field.[26] Such a fit lies well outside the error bars given in Fig. 4(b) (0.25 meV at $B=7$ T and even larger for $B>12$ T), especially in the high magnetic field region where the peak position can be determined very accurately. This remains the case independent from the value of the series resistance and also after considering the uncertainties of the SCR measurements on the shunt. The latter rather tend to make the trace somewhat sublinear, which is even further from the quadratic dependence. From the fit over the linear region we find a slope of 0.18 meV/T. This leads to an effective perpendicular mass $m_{||}$ of 7.3 $m_e$. Since the magnetic field is in the plane of the two-dimensional electron system, $m_{||}$ characterizes the motion perpendicular to this layer. Assuming a plain two-dimensional electron system means that we work in the limit of an infinite electron mass in the perpendicular direction leading essentially to a flat dispersion. Therefore, the huge value for $m_{||}$ seems quite realistic.

If we plot the resistance at a small SD bias of 5 mV as shown in Fig. 5 then we find indeed a linear behavior for large magnetic fields. From the linear fit we can deduce a $B_0$ value of about 2.1–3.7 T. Since we do not know the series resistance exactly, the fit is rather imprecise and yields this rather wide range. Combining this $B_0$ value and the mass $m_{||}$ we find a relaxation time of 1.3–2.3 ps for the onset of Bloch oscillations. Both numbers are a little longer than the 0.8 ps extracted from the position of the NDC peak for zero magnetic field. A comparison of the NDC peak position and height to a two-dimensional transport model[32] that explicitly distinguishes between elastic and inelastic processes allows a more precise analysis. Especially, the model allows for the transfer of energy from the static electric field into the motion perpendicular to the superlattice axis by elastic processes. From this model it is found that elastic scattering by interface roughness dominates with a characteristic time $\tau_e$ of about 300 fs while inelastic scattering by acoustic phonons is very slow at about $\tau_i=20$ ps. The model also states that the position of the NDC peak is determined by the characteristic time $\sqrt{\tau_i \tau} \approx 2.5$ ps, where $\tau=\tau_i\tau_e/(\tau_i+\tau_e)$. The

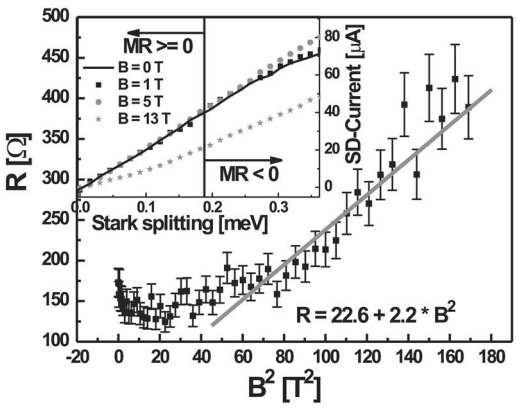


FIG. 5. In the figure the resistance $R=V/I$ for a SD voltage of 5 mV is plotted vs the square of the magnetic field $B$. The gray line indicates a linear fit in the region of large $B$. The inset shows a magnification of the current-voltage data of Fig. 4(a) at low bias, indicating the crossover from positive to negative MR in the limit $B \to 0$.

reason for the difference between the $\tau$ determined from the peak position and that from the experiment lies in the dependence of the NDC peak position on the effective electron temperature. The latter explicitly enters the expression for the drift velocity.[32] When it increases, it shifts the NDC peak to higher fields. Due to the very strong dominance of elastic scattering over the inelastic processes in the SSL the electron temperature can go up to 200 K and thereby shift the peak so that the 2.5 ps result in 0.8 ps assuming a constant electron temperature. The 2.5 ps agree reasonably well with the experimentally extracted numbers. There is actually an additional way to extract an experimental value for $\tau$. As mentioned in Sec. II, the electric field which separates the positive MR region from the negative MR region is in the limit $B \to 0$ given by$F=F_C/2$. The latter is indicated in the inset of Fig. 5 and leads to a $\tau$ of about 2 ps.

In Fig. 6(a) we replot the current-voltage characteristics calculated with the model outlined in Sec. II. However, this time we use $m_{||}=7.3$ $m_e$ and $\tau=0.8$ ps. The latter value is chosen, since it leads to the experimental NDC position at $B=0$. Although a larger $\tau$ is responsible for the onset of Bloch oscillations, we need to use this value for comparison with the experiment. Essentially, we define an effective scattering time which incorporates an increased effective electron temperature. Figure 6(b) shows that now both the peak height and the peak position, which have been scaled to the experimental value at $B=0$, come *quantitatively* very close to the experimental data of Fig. 4. This suggests that the SSL transport can indeed be modeled by the applied semiclassical theory and that electrons inside the SSL do perform stable electrically excited Bloch oscillations.

## V. CONCLUSIONS

The measurements presented in the last section do support the two main conclusions derived from the static transport properties of the shunted SSL structures. The observation of SCRs in the shunt current-voltage characteristics nicely con-

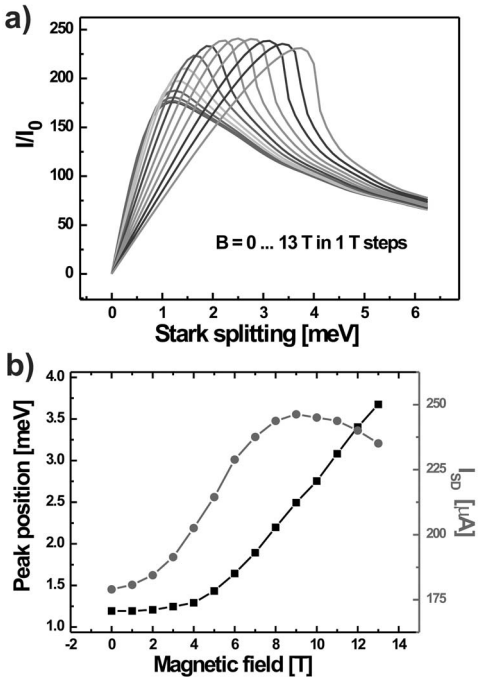


FIG. 6. (a) Numerical results for miniband transport in a superlattice in the presence of a perpendicular magnetic field assuming transport parameters extracted from the experiment. (b) Position and height of the NDC peak in panel (a).

firms that the electric field across the device is indeed very close to homogeneous. The SSL itself shows transport as expected for a superlattice in which electrons perform stable Bloch oscillations even for high densities. The measured current-voltage characteristics exhibit a direct one to one correspondence between the semiclassical drift velocity and the experimentally measured traces. In both a large region of NDC can be observed.

Therefore, we have overcome the problem of electric field instabilities which seriously has hampered the realization of an active two-terminal Bloch oscillator so far. However, since we have achieved the field homogeneity due to the parallel shunt transport, we need to address the question how the shunt changes the gain in the SSL.

The gain in a superlattice structure is based on a negative real part of the dynamic conductivity $\sigma(\omega)$ for all frequencies smaller than the Bloch frequency (cf. Fig. 7). The semiclassical result for its evaluation[2] is in good agreement with quantum mechanical calculations.[8] With the addition of the shunt the relevant conductivity is, due to the parallel alignment of both transport channels, the sum of the dynamic conductivities of SSL and shunt, $\sigma_{tot}(\omega)=\sigma_{SSL}(\omega)+\sigma_{shunt}(\omega)$. So the question arises, whether the shunt contribution diminishes the gain in the SSL. The answer is no, for two reasons. First, the low density, at least two orders of magnitude less than in the SSL, required for the low $nL$ product of the shunt leads to a very small conductivity, resulting in a negligible shift of $\sigma_{tot}(\omega)$. But even more important, the shunt is an almost homogeneous aligned superlattice itself and exhibits itself gain,[10] albeit a very small one. Nevertheless it will add to the SSL gain and might help to overcome unavoidable waveguide losses. Although the gain of the so far realized structures is rather small (cf. Fig. 7), which is also due to the strong dominance of elastic scattering processes combined with small miniband widths, identical structures with wider minibands so that the emission of LO phonons becomes possible are expected to possess gain which exceeds the low temperature values given for the studied samples in Fig. 7 by more than an order of magnitude.

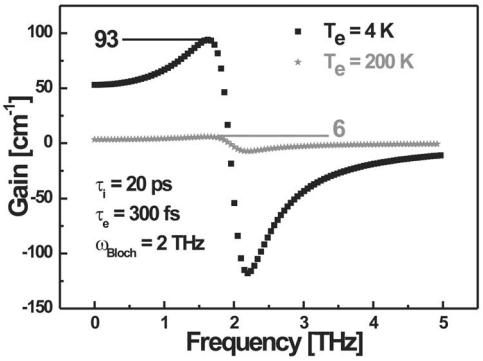


FIG. 7. Gain of an experimentally realized SSL assuming two different effective electron temperatures.

In summary, we have studied the dc transport through a shunted SSL in an external magnetic field. With the magnetic field perpendicular to the electric one, both a highly characteristic crossing of the transport traces and a linear shift of the NDC peak position is observed. The latter represents a clear sign for miniband transport. For the magnetic field parallel to the current, the observation of SCRs confirms that the electric field alignment in our structure is indeed very close to homogeneous. Both facts give strong support to the claim that we have realized a high density SL structure that does not suffer from charge accumulation problems and in which we can electrically excite stable Bloch oscillations.

## ACKNOWLEDGMENTS

We gratefully acknowledge S. J. Allen for helpful discussions and the DFG (SFB348) and the BMBF for financial support.

[1] L. Esaki and R. Tsu, IBM J. Res. Dev. **14**, 61 (1970).
[2] S. A. Ktitorov, G. S. Simin, and V. Y. Sindalovski, Sov. Phys. Solid State **13**, 1872 (1972).
[3] E. E. Mendez, F. Agullo-Rueda, and J. M. Hong, Phys. Rev. Lett. **60**, 2426 (1988).
[4] J. Feldmann, K. Leo, J. Shah, D. A. B. Miller, J. E. Cunningham, T. Meier, G. von Plessen, A. Schulze, P. Thomas, and S. Schmitt-Rink, Phys. Rev. B **46**, R7252 (1992).

[5] C. Waschke, H. G. Roskos, R. Schwedler, K. Leo, H. Kurz, and K. Köhler, Phys. Rev. Lett. **70**, 3319 (1993).
[6] T. Dekorsy, P. Leisching, K. Köhler, and H. Kurz, Phys. Rev. B **50**, R8106 (1994).
[7] K. Unterrainer, B. J. Keay, M. C. Wanke, S. J. Allen, D. Leonard, G. Medeiros-Ribeiro, U. Bhattacharya, and M. J. W. Rodwell, Phys. Rev. Lett. **76**, 2973 (1996).
[8] H. Willenberg, G. H. Döhler, and J. Faist, Phys. Rev. B **67**, 085315 (2003).
[9] Y. Shimada, K. Hirakawa, M. Odnoblioudov, and K. A. Chao, Phys. Rev. Lett. **90**, 046806 (2003).
[10] P. G. Savvidis, B. Kolasa, G. Lee, and S. J. Allen, Phys. Rev. Lett. **92**, 196802 (2004).
[11] T. Feil, H.-P. Tranitz, M. Reinwald, and W. Wegscheider, Appl. Phys. Lett. **87**, 212112 (2005).
[12] E. S. Daniel, B. K. Gilbert, J. S. Scott, and S. J. Allen, IEEE Trans. Electron Devices **50**, 2434 (2003).
[13] V. M. Polyanovskiĭ, Sov. Phys. Semicond. **15**, 1190 (1981).
[14] R. Ferreira, Phys. Rev. B **43**, 9336 (1991).
[15] N. H. Shon and H. N. Nazareno, Phys. Rev. B **53**, 7937 (1996).
[16] N. H. Shon and H. N. Nazareno, Phys. Rev. B **55**, 6712 (1997).
[17] A. Patanè, N. Mori, D. Fowler, L. Eaves, M. Henini, D. K. Maude, C. Hamaguchi, and R. Airey, Phys. Rev. Lett. **93**, 146801 (2004).
[18] B. Movaghar, Semicond. Sci. Technol. **2**, 185 (1987).
[19] D. Miller and B. Laikhtman, Phys. Rev. B **52**, 12191 (1995).
[20] J. Palmier, A. Sibille, G. Etemadi, A. Celeste, and J. Portal, Semicond. Sci. Technol. **7**, B283 (1992).
[21] A. Alexandrou, E. E. Mendez, and J. M. Hong, Phys. Rev. B **44**, 1934 (1991).
[22] L. Canali, M. Lazzarino, L. Sorba, and F. Beltram, Phys. Rev. Lett. **76**, 3618 (1996).
[23] A. Sibille, J. F. Palmier, A. Celeste, J. C. Portal, and F. Mollot, Europhys. Lett. **13**, 279 (1990).
[24] F. Aristone, A. Sibille, J. Palmier, D. Maude, J. Portal, and F. Mollot, Physica B **184**, 246 (1993).
[25] H. J. Hutchinson, A. W. Higgs, D. C. Herbert, and G. W. Smith, J. Appl. Phys. **75**, 320 (1994).
[26] W. Müller, H. T. Grahn, K. von Klitzing, and K. Ploog, Phys. Rev. B **48**, 11176 (1993).
[27] T. Feil, H.-P. Tranitz, C. Gerl, and W. Wegscheider, Proceedings of the 12th International Conference on Modulated Semiconductor Structures (MSS 2005), 2005.
[28] H. L. Stormer, L. N. Pfeiffer, K. W. Baldwin, K. W. West, and J. Spector, Appl. Phys. Lett. **58**, 726 (1991).
[29] A. Sibille, J. F. Palmier, F. Mollot, H. Wang, and J. C. Esnault, Phys. Rev. B **39**, 6272 (1989).
[30] A. Sibille, J. F. Palmier, H. Wang, and F. Mollot, Phys. Rev. Lett. **64**, 52 (1990).
[31] A. Wacker, Phys. Rep. **357**, 1 (2002).
[32] C. Minot, H. L. Person, J. F. Palmier, N. Sahri, F. Mollot, and R. Planel, Semicond. Sci. Technol. **9**, 789 (1994).